A New Assessment of Possible Solar and Lunar Forcing of the Bidecadal Drought Rhythm in the Western United States*

EDWARD R. COOK

Lamont-Doherty Earth Observatory, Columbia University, Palisades, New York

DAVID M. MEKO AND CHARLES W. STOCKTON

Laboratory of Tree-Ring Research, The University of Arizona, Tucson, Arizona

(Manuscript received 6 August 1996, in final form 21 October 1996)

ABSTRACT

A new drought area index (DAI) for the United States has been developed based on a high-quality network of drought reconstructions from tree rings. This DAI is remarkably similar to one developed earlier based on much less data and shows strong evidence for a persistent bidecadal drought rhythm in the western United States since 1700. This rhythm has in the past been associated with possible forcing by the 22-yr Hale solar magnetic cycle and the 18.6-yr lunar nodal tidal cycle. The authors make a new assessment of these possible forcings on DAI using different methods of analysis. In so doing, they confirm most of the previous findings. In particular, there is a reasonably strong statistical association between the bidecadal drought area rhythm and years of Hale solar cycle minima and 18.6-yr lunar tidal maxima. The authors also show that the putative solar and lunar effects appear to be interacting to modulate the drought area rhythm, especially since 1800. These results do not eliminate the possibility that the drought area rhythm is, in fact, internally forced by coupled ocean–atmosphere processes. Recent modeling results suggest that unstable ocean–atmosphere interactions in the North Pacific could be responsible for the drought rhythm as well. However, the results presented here do not easily allow for the rejection of the solar and lunar forcing hypotheses either.

1. Introduction

During the first half of 1996, parts of the western United States were in the grips of a severe drought. This drought, which has now largely abated, extended from the southern Great Plains states of Oklahoma and Texas westward into New Mexico and Arizona. At the time, it was regarded as possibly the worst such event to hit the region since the Dust Bowl years of the 1930s (*New York Times*, 20 May 1996). The timing of its occurrence is interesting because it followed major dry periods in the western United States centered on 1892, 1912, 1934, and 1953 (Borchert 1971), and another serious drought in the mid-1970s. These droughts were all separated by approximately 20–21 yr, and the 1996 drought likewise occurred approximately 20 yr after the 1970s event.

Interest in this apparent bidecadal drought rhythm is understandable because it suggests the presence of some quasi-periodic forcing on the climate system. Should such a forcing exist, its identification could lead to the development of a predictive model for drought in the Great Plains. From the point of view of agricultural production, food supplies and prices, and water resources availability, the ability to predict large-scale droughts some years in advance would be extremely beneficial.

Two external (to the climate system) forcing factors with time constants compatible with the apparent bidecadal drought rhythm have been investigated in the past. These are the 22-yr Hale solar magnetic cycle (Mitchell et al. 1979; Stockton et al. 1983) and the 18.6-yr lunar nodal tidal cycle (Currie 1981, 1984a,b). Each of these studies claims to have found significant statistical links between solar and/or lunar forcing and drought occurrence in the western United States. Yet, claims of this kind are controversial (e.g., Pittock 1978; Briffa 1994), and there is considerable disagreement over the relative merits of the solar and lunar hypotheses as well (e.g., Currie 1984a,b; Stockton et al. 1983). Here, we reexamine these hypotheses using a newly developed high-density grid of long drought reconstructions from tree rings covering the coterminous United States.

Recently, modeling results by Latif and Barnett (1994, 1996), using only the physics of the coupled

*Lamont-Doherty Earth Observatory Contribution Number 5623.

Corresponding author address: Dr. Edward R. Cook, Lamont-Doherty Earth Observatory, Palisades, NY 10964.
E-mail: drdendro@ldeo.columbia.edu

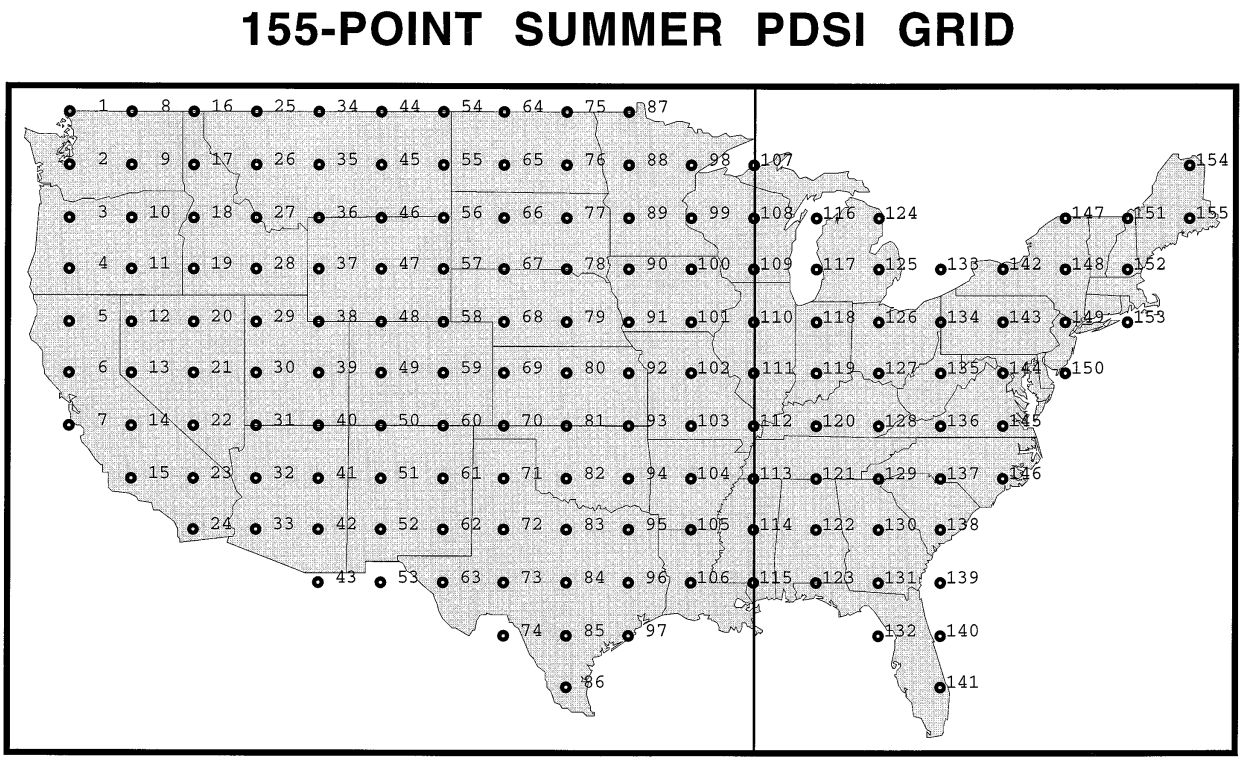

FIG. 1. Map of the PDSI reconstruction grid. The grid spacing is 2° lat × 3° long. There are 155 points on the grid but only 154 PDSI reconstructions. Grid point 141 in southern Florida was not reconstructed. The verticle line through grid points 107–115 separates the western 115-point PDSI grid used for most analyses from the complete grid.

ocean–atmosphere system, have been able to produce a bidecadal cycle in their model runs that extends from the western North Pacific Ocean eastward over the North American continent. Their model does not require any external forcing to generate this cycle in sea surface temperature and atmospheric pressure fields. The statistical results that we will present here are not intended to discount the possibility that the drought rhythm over the western United States is, in fact, internally driven. However, based on our findings here, we do not think that the solar and lunar hypotheses can be summarily rejected at this time either.

2. The drought reconstruction grid

The drought reconstruction grid we will use here for our solar and lunar forcing tests is shown in Fig. 1. It is a 2° lat × 3° long regular grid of 154 time series of summer Palmer Drought Severity Index values (PDSI, Palmer 1965) reconstructed from a network of 425 annual tree-ring chronologies distributed across the United States. Only PDSI grid point 141 in southern Florida could not be reconstructed by tree rings. Otherwise, the grid is complete. The gridpoint reconstructions were created using a principal components regression procedure described in Cook et al. (1996) and cover the common interval 1700–1978. The median PDSI variance explained by tree rings in the calibration period is 54.7% with an interquartile range of 47.4%–63.5%. In the verification period, where tree-ring estimates of PDSI were compared to actual data withheld from the regression model, the explained variance was 36.4% with an interquartile range of 24.3%–49.0%. The westernmost 115 grid points, which will be used for most of the analyses here, have marginally higher calibration and verification statistics. Rotated principal components analysis (Richman 1986) of the grid indicates that the space–time features of drought across the United States (sensu Karl and Koscielny 1983) have been faithfully reproduced in the reconstructions (Cook et al. 1995).

The vertical line in Fig. 1 cutting through grid points 107–115 separates the map along the boundary of the eastern Great Plains. The westernmost 115 grid points will be used for most of our analyses. This region corresponds closely to the western United States region used by Stockton and Meko (1975) and Mitchell et al. (1979) in their studies of past drought from tree rings. Their reconstruction grid was comprised of 40 climatic regions estimated using anywhere from 40 to 65 tree-ring chronologies. In contrast, our western United States grid has almost three times the density of PDSI reconstructions, which are based on 4–5 times as many (mostly new) tree-ring chronologies. Therefore, this assess-

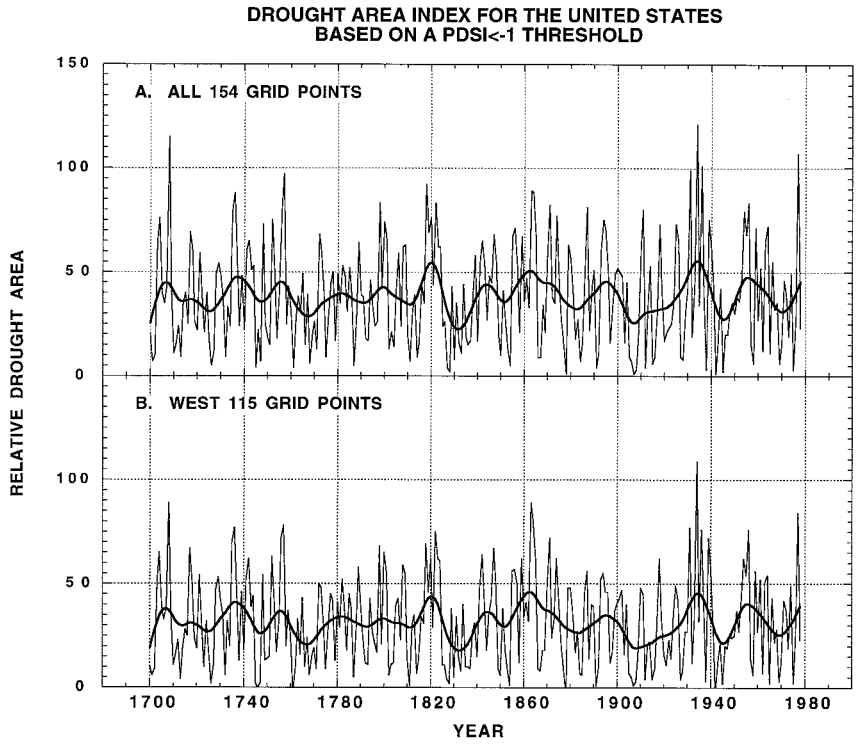

FIG. 2. The DAIs for the complete grid (Fig. 2a) and the 115-point western grid (Fig. 2b) based on a PDSI < -1 threshold.

ment utilizes all new PDSI reconstructions estimated from a largely independent tree-ring dataset.

3. The drought area index

Following the approach taken by Mitchell et al. (1979) in their study of hypothesized solar forcing of rhythmic drought in the western United States, we have developed a new ''family'' of drought area indices (DAI) for the United States. As before, the DAI is simply the count for a given year of the number of gridpoint reconstructions having PDSIs exceeding a given threshold (Stockton and Meko 1975). In the Mitchell et al. (1979) study, three PDSI thresholds were investigated: PDSI < -1 (mild drought or worse), <-2 (moderate drought or worse), and <-3 (severe drought or worse). In this study, we will concentrate on the PDSI < -1.0 threshold because it is less sensitive to spatial variations in explained variance due to regression. However, the results we will show here are essentially unchanged if the PDSI <-2 threshold were used instead.

Mitchell et al. (1979) developed PDSI reconstructions for 40 climatic regions located west of the 90°W meridian based on three relatively sparse, but highly stratified, tree-ring networks composed of 40, 50, and 65 chronologies. Due to the higher density of our PDSI grid, we have 115 grid points covering this same geographic region, plus an additional 39 points covering the United States east of 90°W. Figure 2 shows plots of the annual DAI based on the PDSI < -1 threshold for the full 154 grid points (Fig. 2a) and the reduced set of 115 (Fig. 2b). The 1930s decade, which includes the Dust Bowl years, stands out clearly in both series, and the two series are extremely similar overall ($r = 0.967$). This indicates that the 115 western grid points are contributing overwhelmingly to the DAI variance seen in Fig. 2a. To see why this is so, we have mapped and contoured the number of years at each grid point that have contributed to the DAIs (Fig. 3). Only those regions contributing at least 70 years (i.e., those experiencing at least mild drought ~25% of the time) are contoured. It is apparent that the Great Plains and Rocky Mountains are the most drought prone regions in the United States.

Figure 4 shows the Blackman–Tukey power spectra of the two DAI records. In agreement with the results of Mitchell et al. (1979), each has a statistically significant (a priori $p < .05$) peak with a mean period of 20–23 yr. In addition, significant peaks at 7.8, 4.1, and 2.5 yr are also indicated in our DAI records. The 7.8- and 2.5-yr peaks were also present in some of the power spectra presented by Mitchell et al. (1979). In contrast, their results do not indicate the presence of the 4.1-yr peak, which is most likely related to the El Niño–Southern Oscillation (ENSO). None of the tree-ring networks used by Mitchell et al. (1979) had much coverage in the Texas–Oklahoma region where the ENSO precipitation teleconnection is especially strong (Ropelewski and Halpert

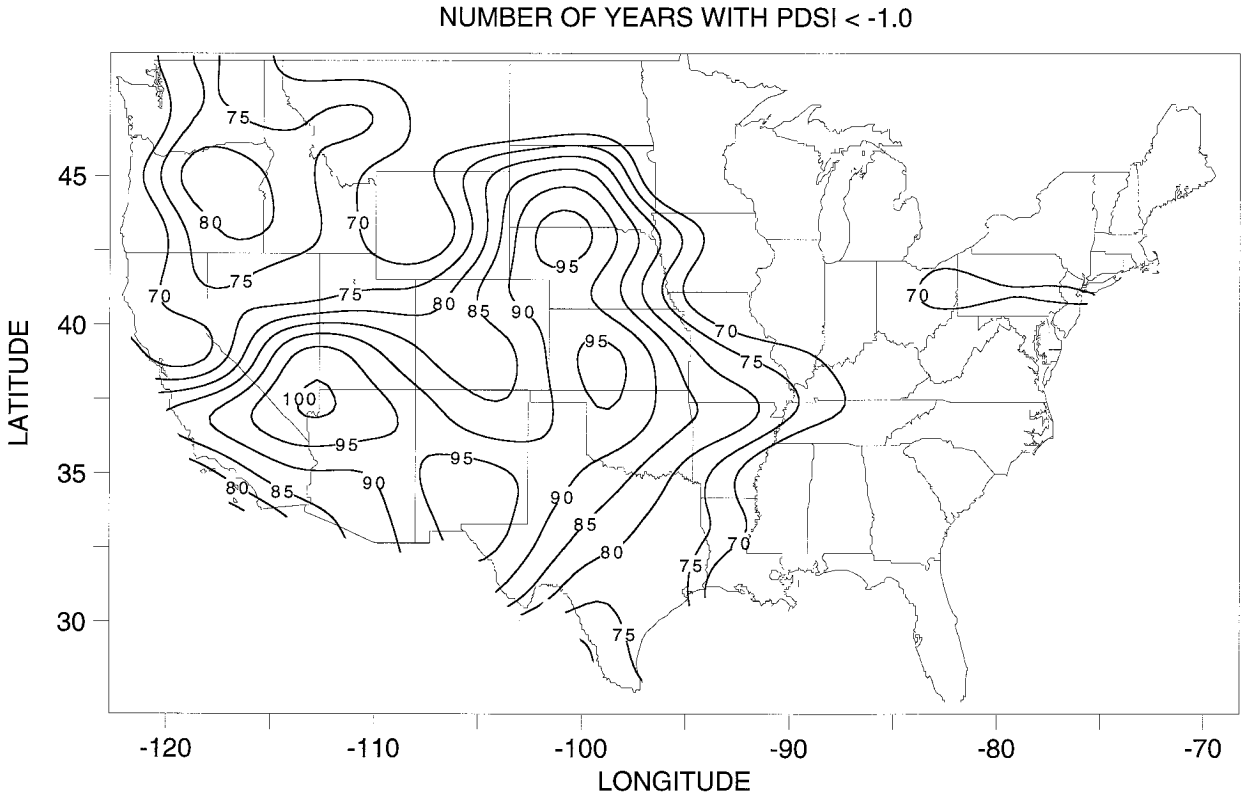

FIG. 3. Map showing the region that contributes most strongly to the DAIs. Only those regions that contributed to at least 70 out of 279 years of DAI are contoured. By this means, the Great Plains and Rocky Mountains states are clearly the most drought prone regions in the United States.

1986; Stahle and Cleaveland 1993). This probably explains why our results differ from theirs in this regard. It is also interesting to note that there is no evidence for an 11-yr peak, which might be associated with the 11-yr sunspot cycle. This putative forcing factor has been associated with patterns of drought and flood in the western United States (Currie 1984b). At the very least, its complete absence in our power spectra, and those in Mitchell et al. (1979), indicates that it does not contribute to spatial variations in drought occurrence in the high drought frequency region shown in Fig. 3.

Given the more complete spatial coverage of our tree-ring network used to reconstruct drought, we believe that our DAI record is a more complete representation of the spectral complexity of the spatial drought signal over the western United States. But overall, our results confirm the long-term existence of a bidecadal drought rhythm in the western United States, with other quasi-periodic components (e.g., Fig. 4) probably contributing as well. Thus, the characteristics of drought revealed in the DAI spectral analyses of Mitchell et al. (1979) appear to be highly robust.

4. Hale solar and lunar nodal tidal forcing of drought

As described earlier, there is some controversy concerning the importance of solar forcing on drought occurrence in the western United States. Mitchell et al. (1979) presented reasonably strong statistical evidence for phase-locking between minima of the 22-yr Hale solar magnetic cycle and epochs of maximum drought area. Specifically, drought area typically peaked approximately 2 yr after the minimum in the Hale solar cycle. This result was consistent back to 1700, except for drought epochs in 1781 and the 1860–1900 period where phase-locking broke down. Currie (1981, 1984a,b) proposed an alternative explanation of the drought rhythm by invoking 18.6-yr periodic lunar nodal tidal and 11-yr solar (sunspot cycle) forcings as the primary mechanisms. In this case, he presented evidence for phase-locking between drought area and lunar tidal maxima. However, he too found that phase-locking broke down, only this time around 1800, such that drought epochs were out of phase before 1800 and in phase after 1800. In a synthesis of these competing hypotheses, Bell (1981a,b) and Stockton et al. (1983) proposed that solar and lunar tidal forcing were together responsible for the observed drought rhythm.

We will examine the solar and lunar tidal hypotheses using the 115 gridpoint DAI record. For this purpose, we will use singular spectrum analysis (Vautard et al. 1992), classical bandpass filtering (Stearns and David 1988), and superposed epoch analysis (Haurwitz and Brier 1981). Singular spectrum analysis has the advantage

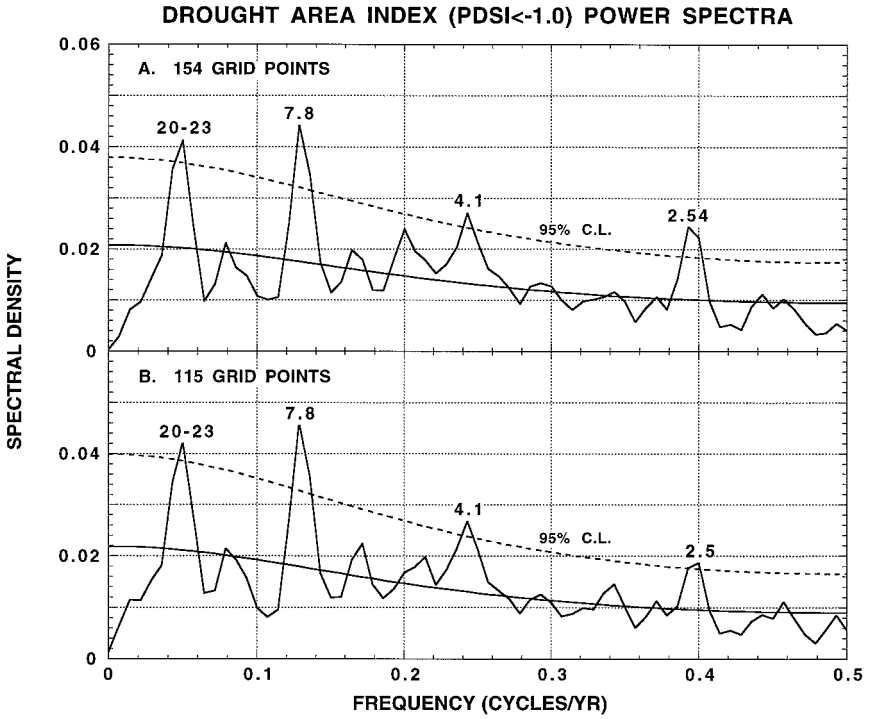

FIG. 4. Blackman–Tukey power spectra of the DAI records shown in Fig. 2. Each spectrum was estimated from 70 lags of the autocovariance function and smoothed with a Hamming window. The resulting spectral estimates have 10 degrees of freedom. The 95% confidence levels are based on first-order Markov null spectra estimated from the data. Significant spectral peaks of 20–23, 7.8, 4.1, and 2.5 yr are indicated in each DAI spectrum.

of being more objective in its extraction of band-limited, oscillatory signals than bandpass filtering because it does not impose an a priori expectation on the data. So, in a sense, singular spectrum analysis is a data-adaptive form of bandpass filtering. On the other hand, this method does not necessarily guarantee the optimal extraction of an oscillatory signal because the operator has very limited control over its frequency response characteristics. This is a clear advantage of bandpass filtering. Superposed epoch analysis provides a means of testing for statistically significant departures in drought areas associated with the timing of solar minima and tidal maxima, which have been associated with western United States drought occurrence.

a. Singular spectrum analysis

Singular spectrum analysis (SSA) is simply the application of empirical orthogonal function (EOF) analysis to the autocovariance matrix of a time series. The EOFs for oscillatory signals come in pairs with nearly equal eigenvalues, and the EOFs themselves are in quadrature with each other (Vautard et al. 1992). So, the total variance associated with an oscillatory signal is the sum of the variances accounted for by the pair of EOFs. The loadings of the EOFs act as bandpass filter weights when applied to the series as described in Vautard et al. (1992). One of the uncertainties in applying SSA is in determining how many lags to use in the autocovariance matrix. Using a window-closing approach, we found that 50 lags produced a very smooth bidecadal waveform without overly smoothing (or bridging) the amplitude modulation apparent in the signal. However, 60 or 70 lags would not have changed the results much in any event. By this we mean that the extracted waveform shown in Fig. 5a was effectively identical to those extracted from autocovariance matrices of 60 and 70 lags. Below 50 lags, the SSA waveform was noticeably less well resolved.

Figure 5a shows the bidecadal waveform of drought as estimated by SSA from a 50-lag autocovariance matrix of the 115-gridpoint DAI. The waveform, which is based on the first two leading EOFs, accounts for approximately 10% of the total variance in DAI. It is apparent that the bidecadal signal in the DAI is somewhat amplitude modulated with peak amplitudes in the 1735–70, 1815–60, and 1920–70 periods that average about ± 10 DAI units. In terms of area affected by drought, an increase of 10 DAI units is equivalent to 10 additional grid points with PDSI < -1. This equates to a drought area expansion or contraction of approximately 500 000 km^2. So, these changes are not trivial, especially if they involve contiguous grid points. Periods of reduced amplitude are indicated for the 1700–30, 1770–90 (weakly so), and

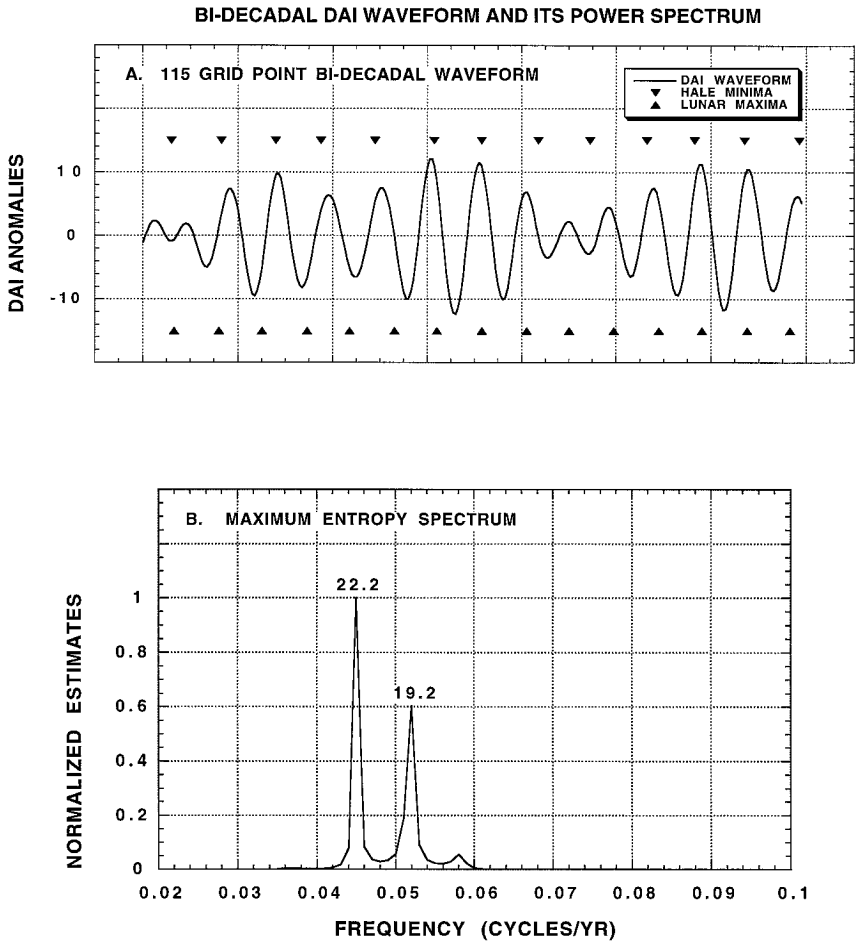

FIG. 5. The DAI bidecadal waveform extracted by SSA (Fig. 5a) based on an order-50 autocovariance matrix. The units are DAI anomalies from the long-term mean. Above and below the waveform are symbols showing the years of Hale solar minima (▼) and lunar tidal maxima (▲), respectively. Some phase-locking with the DAI bidecadal signal is indicated. The MEM spectrum of the SSA waveform is based on an order-50 PEF. This spectrum indicates the presence of a primary 22.2-yr peak and a secondary 19.2-yr peak, which are close to the Hale solar and lunar tidal periods.

1870–1910 periods, with values that average about ±5 DAI units.

The maximum entropy method (MEM) of spectral analysis (Marple 1987) was used to describe the frequency domain properties of the bidecadal waveform. Applying MEM to SSA waveforms is advantageous because the prefiltered waveforms have higher signal-to-noise ratios, thereby reducing the length of the prediction error filters (PEF) needed to resolve certain spectral peaks (Penland et al. 1991). This in turn reduces the number of spurious spectral peaks in MEM spectra caused by overly long PEFs. Figure 5b shows the MEM spectrum of the DAI bidecadal waveform based on an order-50 PEF. It has two peaks, one at 22.2 yr and a lesser one at 19.2 yr. The former agrees closely with the mean period of the Hale solar magnetic cycle and the results of Mitchell et al. (1979), while the latter is reasonably close to the 18.6-yr lunar tidal cycle and the results of Currie (1984a). Our Blackman–Tukey spectral analyses (Fig. 4) were incapable of resolving these spectral peaks. Hence, the mean period found by that method was 20 yr, with some clear asymmetry in the peak favoring added power at around 22 yr.

Our MEM result is similar to that found by Bell (1981b), also using MEM, and Stockton et al. (1983) using a different method of high-resolution spectral analysis. It is also free from any a priori decisions concerning the choice of bandpass filters used to extract the waveform, that is, we have not potentially imposed any oscillatory or periodic properties on the data through the use of 22-yr or 18.6-yr bandpass filters.

The relationship between the bidecadal DAI oscillations and the timing of Hale solar minima (▼) and lunar tidal maxima (▲) are indicated in Fig. 5a. In 10 out of 13 cases, DAI follows Hale minima by about 1–2 yr, a result nearly identical to that of Mitchell et al. (1979).

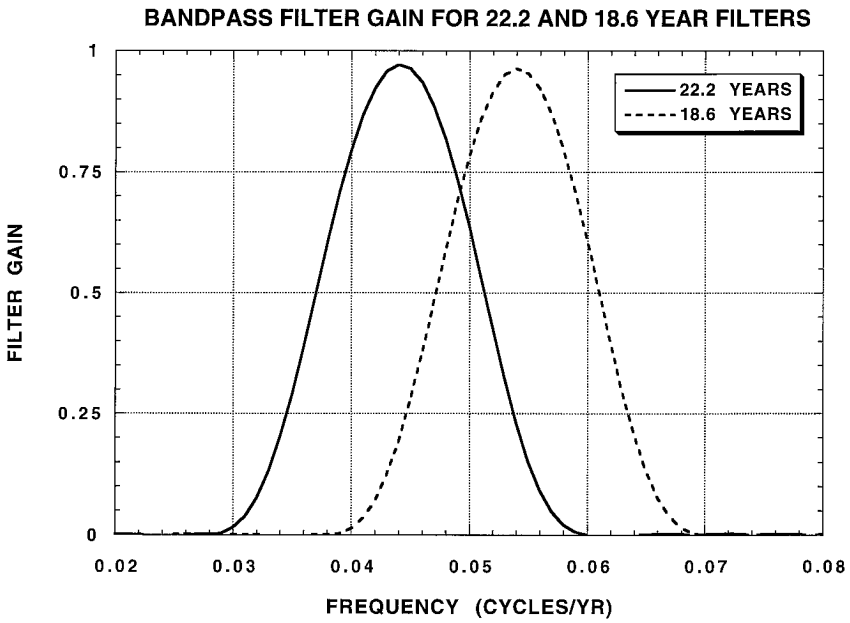

FIG. 6. The filter gains of the 22.2- and 18.6-yr bandpass filters used here. The gains overlap somewhat, resulting in the filtered series not being orthogonal.

There are also two periods where this apparent phase-locking breaks down, one in the 1700–30 period and the other in the 1860–1900 period. The latter result agrees again with that of Mitchell et al. (1979). The relationship between lunar tidal maxima and DAI also follows that reported by Currie (1984a). That is, before 1800 the relationship is clearly out of phase by nearly a half-cycle on average. This is followed by an apparent phase discontinuity around 1800 that locks the relationship into phase for the remainder of the record. So, we can see that the 115-gridpoint DAI record has been able to reproduce virtually all of the contentious characteristics described earlier.

Up to this point, our results indicate that the 22-yr Hale solar cycle and the 18.6-yr lunar tidal cycle may both be contributing to drought occurrence in the western United States. This joint forcing on the bidecadal timescale was first suggested by Bell (1981a,b) and later verified by Stockton et al. (1983). Indeed, the association between Hale sunspot minima and drought area appears to be quite strong since 1730, the major exception being the 1860–1900 period where the phase-locking disappears. In contrast, phase-locking with the 18.6-yr lunar tidal cycle is essentially bimodal, with a major phase discontinuity occurring around 1800. Currie (1984a,b) argues that this is simply an expression of a nonlinear system that allows for such ''bistable phasing.'' Currie (1984b) also argues that there is no phase-locking with the Hale solar cycle at all since the mid-nineteenth century. However, our results (e.g., Fig. 5a) and the results of Mitchell et al. (1979) clearly suggest that phase-locking with the Hale cycle has existed since 1900. In any case, the Hale solar cycle length has shortened to only about 21 yr in length during the twentieth century, making it more difficult to distinguish from the lunar tidal cycle after only four cycles up to 1978.

b. Bandpass filtering

The DAI appears to contain two band-limited, roughly bidecadal, signals that help drive drought area changes in the western United States. To investigate these signals more discretely, we have applied narrow bandpass filters to the DAI series centered on 22.2 and 18.6 yr. The filter gains for these two filters are shown in Fig. 6. Because of the closeness of the periods being studied, the gains overlap somewhat and the resulting filtered series are not orthogonal. However, most of the variance passed by each filter (~66%) is unique. Figure 7 shows the 22.2- and 18.6-yr waveforms extracted by the bandpass filters. Each shows characteristics that have been discussed before. First, each filtered series again shows some evidence for phase-locking with its respective forcing factor. This might be expected because the bandpass filters have forced them to be that way. Second, the phase shifts in the DAI relationship with solar and lunar forcing are again evident, especially the phase discontinuity in the 18.6-yr signal.

The sum of the 22.2- and 18.6-yr waveforms is shown in Fig. 8a. It has been rescaled to have the same amplitude as the waveform extracted by SSA. This was done to correct for the lack of orthogonality between the waveforms caused by the overlapping filter gains. The correlation between the SSA waveform in Fig. 5a and the sum in Fig. 8a is 0.996, indicating that the combined bandpass filter waveforms are an accurate expression of

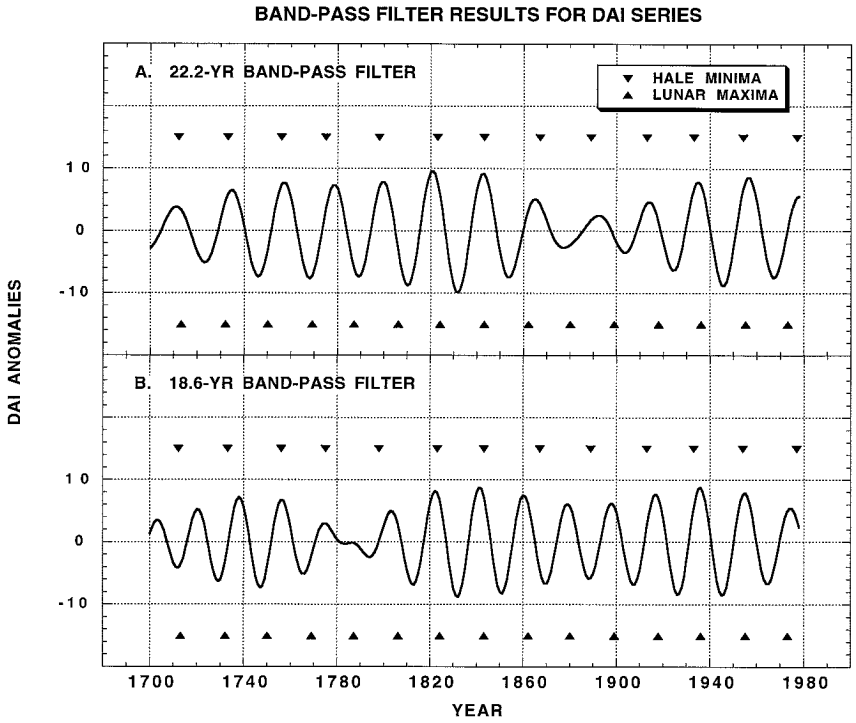

FIG. 7. The 22.2- and 18.6-yr waveforms estimated by the bandpass filters. The waveforms have a correlation of 0.58, meaning that approximately 66% of the variance between them is unique. Years of solar minima and tidal maxima are indicated as before.

the SSA composite signal. As an experiment, equal-amplitude sine waves with periods of 22.2 and 18.6 yr were also generated for comparison. To make these theoretical processes compatible with the actual waveforms, their initial phases were set by the first minimum (1711.5) and maximum (1712.8) of the solar and lunar tidal cycles, respectively. Then, the theoretical signals were summed and rescaled to the same amplitude as the actual sum. Finally, the theoretical sum was shifted back 20 yr to achieve a better visual alignment with the actual sum.

This theoretical sum, shown in Fig. 8b, is at best only a rough approximation of reality because the Hale solar cycle is quasi-periodic, and it assumes that both solar and lunar forcing are equal in strength. Yet, there are some remarkable similarities between the actual and theoretical waveforms. In particular, the amplitude modulation seen in the actual sum is reproduced almost exactly from 1800 to 1978 in the theoretical sum. This includes the 1860–1900 period when phase-locking between DAI and the Hale solar cycle broke down. Thus, this loss of phase-locking appears to have been caused by interference with the 18.6 lunar tidal cycle, an event that ought to happen every 114.7 yr as part of the beat frequency, or interference pattern, between the two harmonics. This possibility was first suggested by Bell (1981a). Prior to 1800, the modulation of the theoretical sum is largely out of phase with the actual waveform, for example, in the 1700–30 period. This early period is a time when solar variability was just emerging from the Maunder Minimum of little or no sunspot activity (Eddy 1976; Hoyt and Schatten 1993), so the assumption of constant solar forcing is clearly suspect there. However, if we take into account the phase shift in the 18.6-yr cycle prior to 1800 by simply shifting that segment back one-half cycle and filling in the gap with zeroes, the agreement between actual and theory improves considerably. This result is shown in Fig. 8c. So, the amplitude modulation in the bidecadal drought rhythm waveform may be explained simply by constructive and destructive interference between the solar and lunar terms, with a phase shift in the lunar forcing component prior to 1800 changing the pattern of interference and resulting modulation.

The relatively good match between the actual and theoretical modulation envelopes in Figs. 8a and 8c supports the argument that the bidecadal drought rhythm in the western United States is related to combined solar and lunar tidal forcing. How the two are physically related is unknown, but they do appear to be statistically additive, which implies that they are physically decoupled (Stockton et al. 1983).

5. Superposed epoch analysis

Superposed epoch analysis (SEA) has been used frequently in the past to search for sun–climate connections (Haurwitz and Brier 1981). In the context of this paper, SEA basically takes a climatic time series and cuts it up into a group of subseries, with leads and lags centered

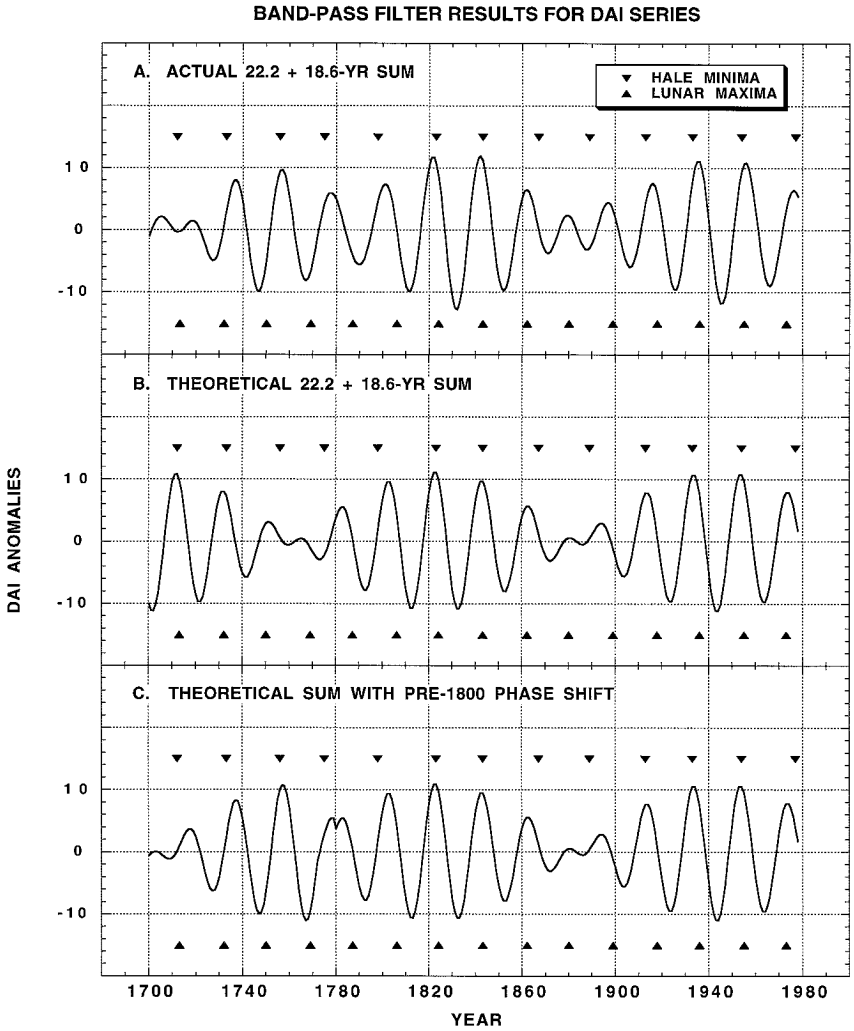

FIG. 8. (a) The sum of the actual bandpass-filtered waveforms and two equal-amplitude theoretical sine waves with periods of 22.2 and 18.6 yr (b) without and (c) with the pre-1800 phase discontinuity. Each has been rescaled to have the same amplitude as the SSA waveform. Note the similar amplitude modulation in both the actual and theoretical sums, especially after the phase discontinuity around 1800 is taken into account. Years of solar minima and tidal maxima are indicated as before.

in time around key years, or epochs, of a criterion variable that may be causally related to climate. The epochs may be dates of sunspot minima, lunar tidal maxima, or volcanic eruptions, for example. The resulting group of climate subseries, centered on the epochs, are averaged together in an effort to see if any of the resulting means are statistically different than zero. Although a standard *t* test could be used to test the means in this way, Haurwitz and Brier (1981) recommend a Monte Carlo method for testing significance based on randomly shuffling the dates of the epochs. This is the method we have used here.

In our study, we developed DAI composites based on leading and lagging the unfiltered and filtered indices ± 10 yr around the dates of Hale sunspot minima and lunar tidal maxima. These dates have been taken from Mitchell et al. (1979) and Currie (1984b). Following Haurwitz and Brier (1981), we generated 95% and 99% empirical confidence limits by shuffling the key year dates 5000 separate times to generate the suite of randomized composites needed for calculating the Monte Carlo confidence limits. We have done this for the raw DAI series (Fig. 1b), the DAI waveform from SSA (Fig. 5a), and the bandpass-filtered waveforms (Figs. 7a,b).

Figure 9 shows the SEA results using the Hale solar minima as the key years. The raw DAI plot indicates a somewhat weak linkage between DAI and the Hale solar cycle, with the strongest association occurring 3 yr prior to the minima on average. Significant secondary peaks of association occur in $t = 0$ (no lag) and $t + 2$ yr. The latter finding is similar to that found by Mitchell et al. (1979) based on their bandpass-filtered data. The SEA plots for the filtered series are much smoother, as they

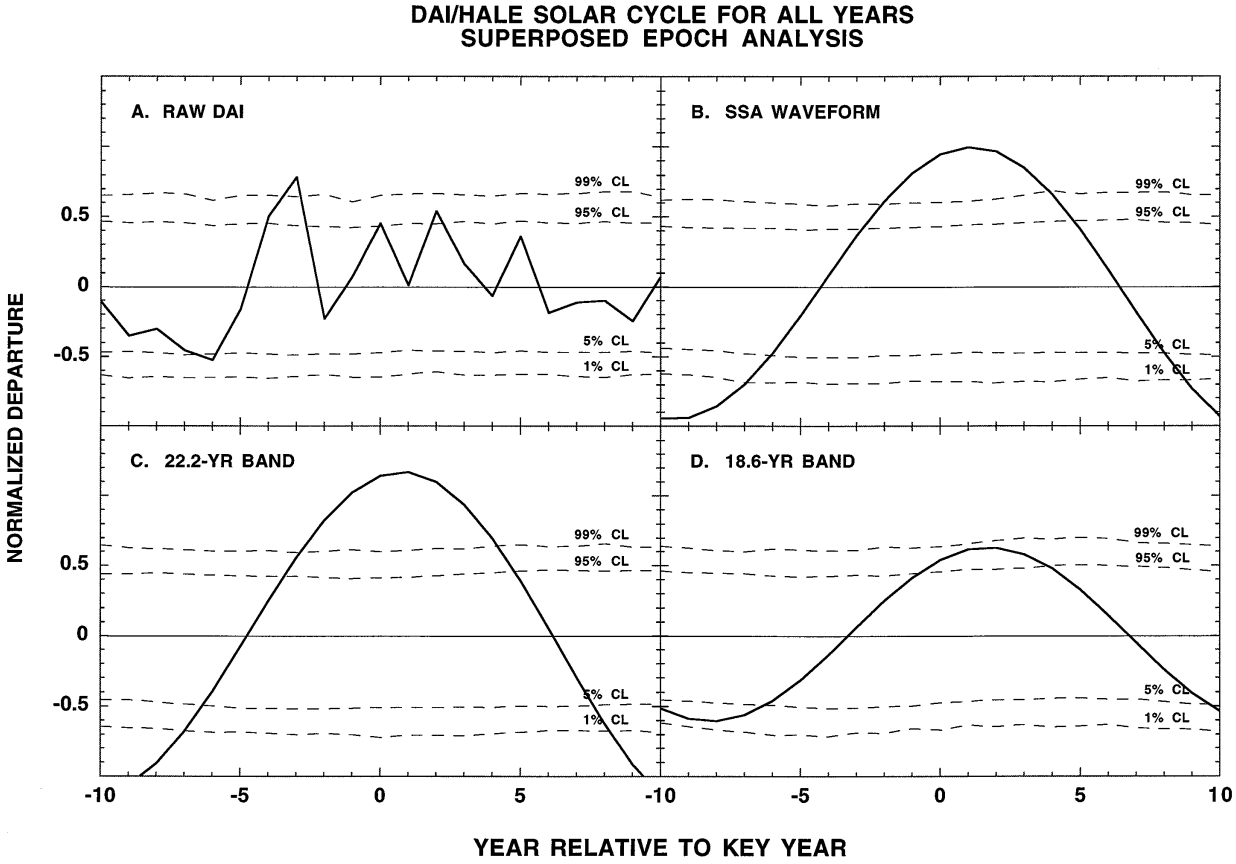

FIG. 9. SEA results for the raw DAI series and the SSA and bandpass-filtered waveforms using all of the Hale solar minima dates since 1700 as key years. The SEA units are standard normal deviates. The confidence limits are based on randomly shuffling the key years 5000 times.

must be. The SSA and 22.2-yr composites are very similar and strongly significant in year $t + 1$. This result further validates the presence of a 22-yr cycle in the DAI data. The 18.6-yr composite has an understandably weaker link to the Hale cycle because most of the 22-yr component in the DAI was removed by bandpass filtering. Even so, it is weakly significant in years $t + 1$ and $t + 2$. This result illustrates the difficulty in cleanly separating the 22.2- and 18.6-yr effects because they will often be nearly in phase (e.g., the solar/lunar key years in the twentieth century are 1913.2/1917.5, 1933.4/1936.1, 1954.1/1954.7, and 1976.8/1973.3, a mean difference of -0.72 yr). In any case, the precision of the PDSI estimates used in the calculating the DAI may not be high enough to cleanly differentiate the two signals.

Figure 10 shows the SEA results using the dates of lunar tidal maxima as the key years. In the raw DAI plot, there is almost nothing significant to be found. However, both the SSA and 18.6-yr waveforms show some evidence for phase-locking 1 yr prior to the maxima, a result that supports the existence of this effect on DAI as well. The result for the 22.2-yr band is weaker still than that shown in Fig. 9d for the 18.6-yr band, but there is still a tendency for the association to strengthen near year t-1.

It can be argued that the lunar tidal SEA results in Fig. 10 are overly weak because we have not taken into account the 1800 phase discontinuity pointed out by Currie (1984a). Of course, the same argument could also be made about the Hale solar SEA results because of the phase-locking breakdown in the 1860–1900 period. To see how that might be so, we redid the solar and lunar SEAs after deleting the necessary key years in the respective offending periods. This reduced the number of solar key years from 13 to 11 and lunar key years from 15 to 10.

Figures 11 and 12 show these results. Not surprisingly, the SEA results have strengthened in each case. In Figure 11, there is now a stronger link between raw DAI and the Hale cycle in year $t + 2$, and the SSA and 22.2-yr band results have also strengthened slightly. Interestingly, even the 18.6-yr DAI band shows improved association with the Hale solar cycle. The lunar tidal results in Fig. 12 show similar improvements for the raw DAI, and the SSA and 18.6-yr waveforms as well. In addition, the 22.2-yr band result has also improved over that in Fig. 10.

The improvements seen in the 18.6-yr band based on solar key years and the 22.2-yr band based on lunar key

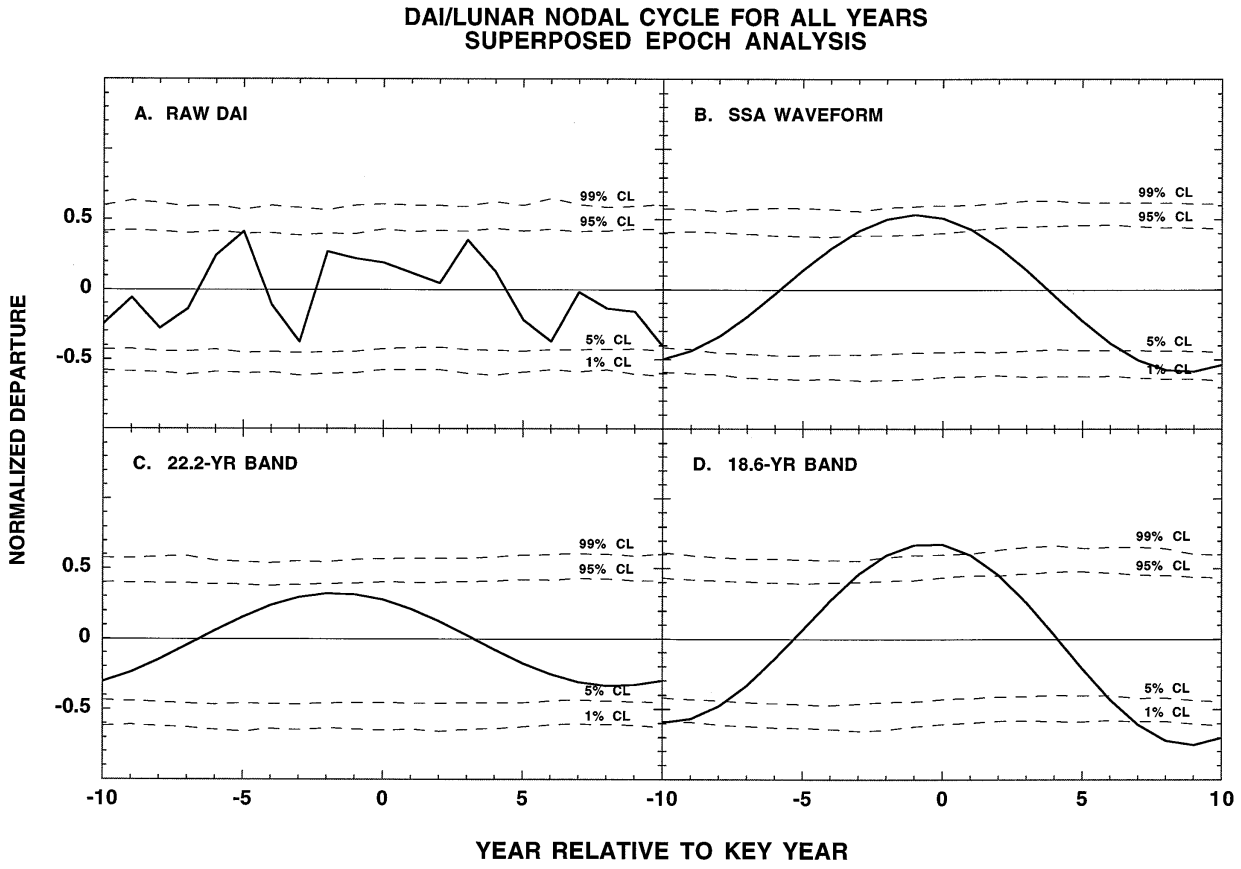

FIG. 10. SEA results for the raw DAI series and the SSA and bandpass-filtered waveforms using all of the lunar nodal tidal maxima dates since 1700 as key years. See the Fig. 9 caption for more details.

years again emphasizes the difficulty of cleanly disassociating the 22.2- and 18.6-yr cycles in the DAI analyses. Thus, the Hale solar and lunar tidal cycles appear to have interacted significantly with DAI in the western United States over the past three centuries. Regardless, we find no basis for Currie's (1984a) claim that the Hale solar cycle ceases to be a factor after 1800. Except for the phase breakdown in the 1860–1900 period, which was apparently caused by destructive interference with the 18.6-yr cycle, DAI remains phase-locked with the Hale solar cycle since 1800 at a level comparable to that seen with the lunar tidal cycle.

6. Discussion

The results of this study into the possible connection between the bidecadal drought rhythm in the western United States and solar and lunar tidal forcing indicate the following.

1) The DAI, first developed and analyzed by Stockton and Meko (1975) and Mitchell et al. (1979), is a robust expression of the spatial variability of drought occurrence in the western United States.
2) The bidecadal drought rhythm is a long-term feature of drought occurrence since 1700.
3) SSA, bandpass filtering, and SEA of the DAI record all indicate some phase-locking with Hale solar cycle minima and lunar tidal maxima.
4) Solar and lunar forcing appear to interact additively to modulate the DAI, especially if the pre-1800 phase discontinuity in the lunar term is considered.

None of the results presented here should be construed as implying physical proof that solar and/or lunar forcing of drought is operating in the western United States. On the other hand, the statistical evidence for these forcings appears to be strong enough to justify the continued search for a physical model that could explain these apparent linkages. O'Brien and Currie (1993) have attempted to do so for the lunar nodal cycle, while Rind and Overpeck (1993) have used general circulation models to explore the potential forcing due to solar variability at century timescales.

O'Brien and Currie (1993) argue that the sensitivity of atmospheric circulation and pressure fields to lunar tidal forcing is due to the nonequilibrium state of the atmosphere and resulting pressure gradients. They use a

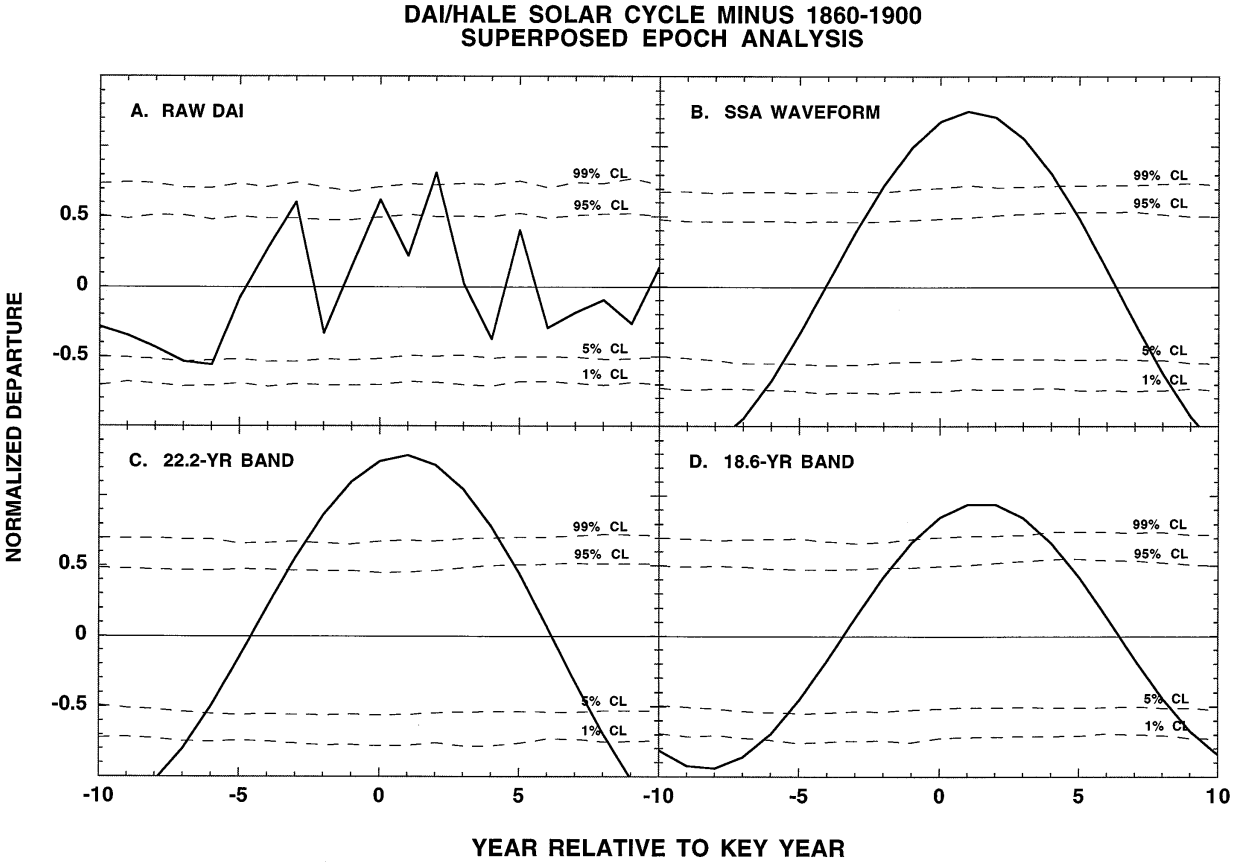

FIG. 11. SEA results for the raw DAI series and the SSA and bandpass-filtered waveforms after deleting the Hale solar minima dates in the 1860–1900 period. Predictably, the results are stronger than those in Fig. 9. See the Fig. 9 caption for more details.

number of theoretical arguments to explain the spatial and temporal properties of the lunar tidal waveforms extracted from climatic and tree-ring time series around the world. Among other things, they argue that the 18.6-yr signal is amplitude modulated by atmospheric factors that modify the east–west and north–south wind systems. These wind systems in turn modify the amplitudes and horizontal wavelengths of the 18.6-yr signals (O'Brien and Currie 1993). However, as we have shown here, the amplitude modulation in the DAI waveform may also be explained by the simple linear interaction between Hale solar and lunar tidal forcing.

Rind and Overpeck (1993) ran a coarse-resolution (8° lat × 10° long) general circulation model (GCM) in which solar forcing at the top of the atmosphere was reduced by 0.25%. This reduction was equal to that suggested by Lean et al. (1992) for the Maunder minimum period of little or no sunspot activity in the seventeenth century. The coarseness of this GCM precludes a detailed examination of the climatic impact of the solar forcing reduction over North America. However, North America and nearby oceanic regions showed some of the largest changes in annual temperature, sea level pressure, and precipitation over the globe, including a reduction in precipitation in the western region (Rind and Overpeck 1993, their Fig. 6). In an independent GCM experiment, Nesme-Ribes and Ferreira (1993) also found that the midlatitudes of North America were much drier during the winter season when solar irradiance was reduced to Maunder Minimum levels. None of these GCM experiments attempted to directly model changes in climate that might be due to the smaller changes in radiative forcing (~0.10%) associated with the 11-yr or 22-yr solar cycles. Such changes in radiative forcing are generally considered too small to be seen in GCM experiments due to the thermal inertia of the oceans (Wigley and Raper 1990). Regardless, the GCM results based on a ''Maunder Minimum'' reduction in solar forcing suggest that North America may be one of the more sensitive regions worldwide to changes in solar irradiance associated with sunspot activity.

As noted earlier, Latif and Barnett (1994, 1996) have produced a bidecadal oscillation in a coupled ocean–atmosphere model, which orginates from unstable ocean–atmosphere interactions in the North Pacific. Since this oscillation arises without the need for any external forcing, it is still possible that the western United States drought rhythm is due solely to the internal dynamics of the ocean–atmosphere system. Given the similar time constants of the solar, lunar, and internally driven oscil-

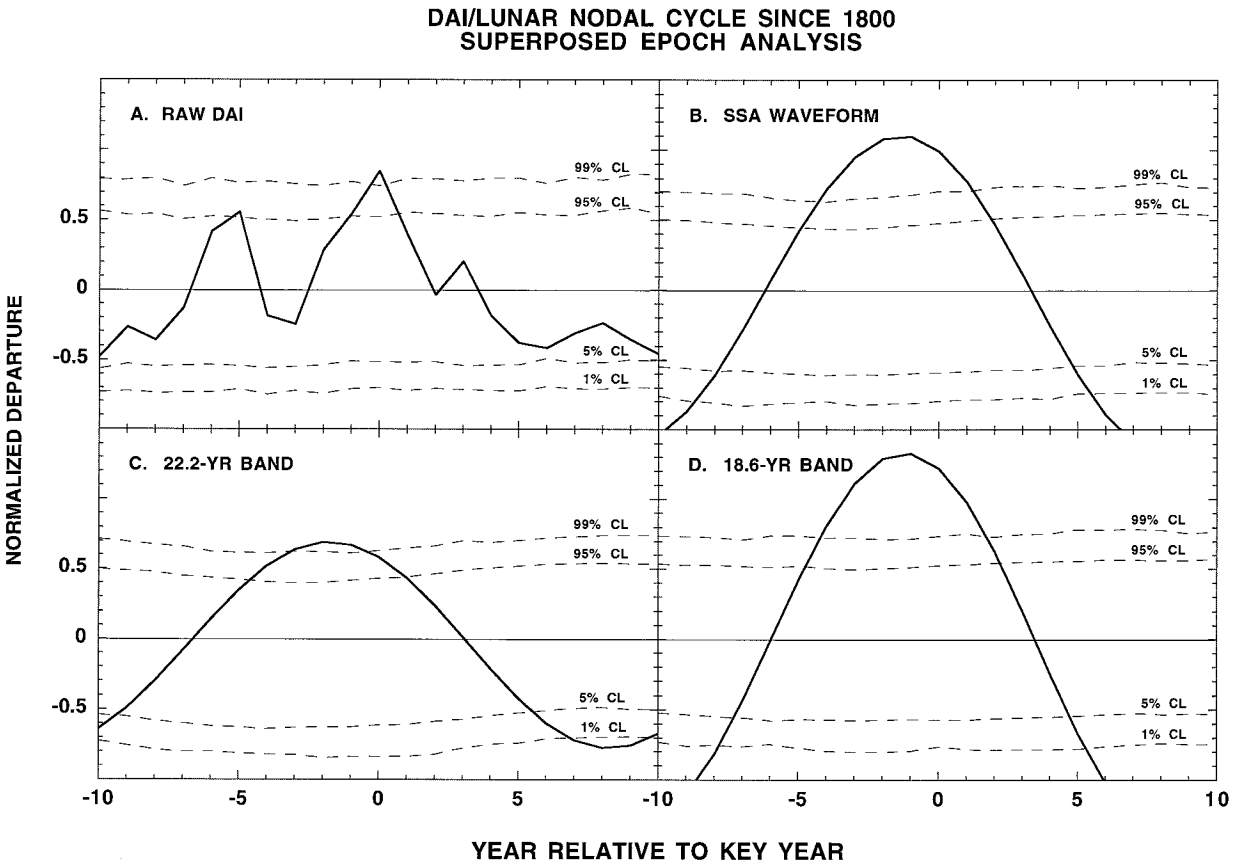

FIG. 12. SEA results for the raw DAI series and the SSA and bandpass-filtered waveforms after deleting the pre-1800 lunar nodal tidal maxima dates. Predictably, the results are stronger than those in Fig. 10. See the Fig. 9 caption for more details.

lations, it may be very difficult to statistically differentiate them in the drought data to the degree necessary to identify which is (are) the true cause(s). Presumably, some kind of unique ''fingerprint'' in the response pattern of drought over North America would be necessary to do so, something that is not yet available.

The apparent similarity between the modulation envelope of the bidecadal DAI signal and that expected from a simple linear interaction between the solar and lunar forcings suggests that they may be responsible for the observed bidecadal drought rhythm. However, the theoretical modulation envelope varies with a period of approximately 115 yr, so it is difficult to be very confident with only 279 yr of data for comparison. Extending these DAI analyses back to 1600 or earlier, as Mitchell et al. (1979) did, would clearly be worthwhile. This will be possible in many parts of the western United States grid. Regardless, until the bidecadal drought rhythm is shown to arise exclusively from something akin to the Latif–Barnett mode of internal forcing, the solar and lunar hypotheses will be difficult to reject.

Latif and Barnett (1996) suggest that their internally driven cycle has the potential for long-range climate forecasting over North America. To the degree that the bidecadal drought rhythm persists in the future as it has in the past, our results also suggest this possibility. The DAI record used by Mitchell et al. (1979) ended in 1962. From their results alone, it would have been reasonable to forecast droughts in the 1970s and 1990s. As noted earlier, a drought did occur in the mid-1970s and the 1996 drought occurred more or less on cue in the mid-1990s. So, the potential for useful forecasts of the drought rhythm appears to be promising. Unfortunately, the ''bistable'' phasing of lunar forcing presents a serious problem for any forecasting model. The phase discontinuities presumably occur as random events, making them essentially unpredictable. Therefore, any operational forecast of drought could be seriously degraded by this abrupt change of phase in the future.

The spectrum of the DAI contains more than just a bidecadal rhythm. The 7.8-yr peak noted earlier is comparable in magnitude to the ~20-yr peak and accounts for an additional 10% of the DAI variance. This suggests that multiyear forecasting skill could be improved significantly by including the 7.8-yr term in the model. This could be easily done if the forecast model of DAI is purely stochastic. Experiments to quantify the potential forecast skill of the DAI using the bidecadal and 7.8-yr quasi-periodicities have not yet been done, however.

Acknowledgments. This study was made possible through the support by the NOAA Office of Global Programs Paleoclimatology Program Grant NA36GP0139.

REFERENCES

Bell, P. R., 1981a: The combined solar and tidal influence on climate. *Variations of the Solar Constant,* S. S. Sofia, Ed., National Aeronautics and Space Administration, 241–256.

——, 1981b: Predominant periods in the time series of drought area index for the western high plains AD 1700 to 1962. *Variations of the Solar Constant,* S. S. Sofia, Ed., National Aeronautics and Space Administration, 257–264.

Borchert, J. R., 1971: The Dust Bowl in the 1970s. *Ann. Assoc. Amer. Geogr.* **61,** 1–22.

Briffa, K. R., 1994: Grasping at shadows? A selective review of the search for sunspot-related variability in tree rings. *The Solar Engine and Its Influence on Terrestrial Atmosphere and Climate,* E. Nesme-Ribes, Ed., NATO ASI Series, Vol. I 25, Springer-Verlag, 417–434.

Cook, E. R., D. M. Meko, D. W. Stahle, and M. K. Cleaveland, 1995: Reconstruction of past drought across the coterminous United States from a network of climatically sensitive tree-ring data. NOAA Office of Global Programs Final Rep., 48 pp.

——, ——, ——, and ——, 1996: Tree-ring reconstructions of past drought across the coterminous United States: Tests of a regression method and calibration/verification results. *Tree Rings, Environment and Humanity,* J. S. Dean, D. M. Meko, and T. W. Swetnam, Eds., Radiocarbon, 155–169.

Currie, R. G., 1981: Evidence for 18.6 year M_N signal in temperature and drought conditions in North America since A.D. 1800. *J. Geophys. Res.,* **86,** 11 055–11 064.

——, 1984a: Evidence for 18.6-year lunar nodal drought in western North America during the past millennium. *J. Geophys. Res.,* **89,** 1295–1308.

——, 1984b: Periodic (18.6-year) and cyclic (11-year) induced drought and flood in western North America. *J. Geophys. Res.,* **89,** 7215–7230.

Eddy, J. A., 1976: The Maunder Minimum. *Science,* **192,** 1189–1202.

Haurwitz, M. W., and G. W. Brier, 1981: A critique of the superposed epoch analysis method: Its application to solar-weather relations. *Mon. Wea. Rev.,* **109,** 2074–2079.

Hoyt, D. V., and K. H. Schatten, 1993: A discussion of plausible solar irradiance variations, 1700–1992. *J. Geophys. Res.,* **98,** 18 895–18 906.

Karl, T. R., and A. J. Koscielny, 1983: Drought in the United States. *J. Climatol.,* **2,** 313–329.

Latif, M., and T. P. Barnett, 1994: Causes of decadal climate variability over the North Pacific and North America. *Science,* **266,** 634–637.

——, and ——, 1996: Decadal climate variability over the North Pacific and North America: Dynamics and predictability. *J. Climate,* **9,** 2407–2423.

Lean, J., A. Skumanich, and O. R. White, 1992: Estimating the sun's radiative output during the Maunder Minimum. *Geophys. Res. Lett.,* **19,** 1591–1594.

Marple, S. L., Jr., 1987: *Digital Spectral Analysis with Applications.* Prentice-Hall, 289 pp.

Mitchell, J. M., Jr., C. W. Stockton, and D. M. Meko, 1979: Evidence of a 22-year rhythm of drought in the western United States related to the Hale solar cycle since the 17th century. *Solar-Terrestrial Influences on Weather and Climate,* B. M. McCormac and T. A. Seliga, Eds., D. Reidal, 125–144.

Nesme-Ribes, E., and E. N. Ferreira, 1993: Solar dynamics and its impact on solar irradiance and the terrestrial climate. *J. Geophys. Res.,* **98,** 18 923–18 935.

O'Brien, D. P., and R. G. Currie, 1993: Observations of the 18.6-year cycle of air pressure and a theoretical model to explain certain aspects of this signal. *Climate Dyn.,* **8,** 287–298.

Palmer, W. C., 1965: Meteorological drought. Weather Bureau Research Paper 45, 58 pp.

Penland, C., M. Ghil, and K. M. Weickmann, 1991: Adaptive filtering and maximum entropy spectra with application to changes in atmospheric angular momentum. *J. Geophys. Res.,* **96,** 22 659–22 671.

Pittock, A. B., 1978: A critical look at long-term sun–weather relationships. *Rev. Geophys. Space Phys.,* **16,** 400–420.

Richman, M. B., 1986: Rotation of principal components. *J. Climatol.,* **6,** 293–335.

Rind, D., and J. Overpeck, 1993: Hypothesized causes of decade-to-century climate variability: Climate model results. *Quat. Sci. Rev.,* **12,** 357–374.

Ropelewski, C. R., and M. S. Halpert, 1986: North American precipitation and temperature patterns associated with the El Niño/Southern Oscillation (ENSO). *Mon. Wea. Rev.,* **114,** 2352–2362.

Stahle, D. W., and M. K. Cleaveland, 1993: Southern Oscillation extremes reconstructed from tree rings of the Sierra Madre Occidental and southern Great Plains. *J. Climate,* **6,** 129–140.

Stearns, S. D., and R. A. David, 1988: *Signal Processing Algorithms.* Prentice-Hall, 257 pp.

Stockton, C. W., and D. M. Meko, 1975: A long-term history of drought occurrence in western United States as inferred from tree rings. *Weatherwise,* **28,** 244–249.

——, J. M. Mitchell Jr., and D. M. Meko, 1983: A reappraisal of the 22-year drought cycle. *Solar-Terrestrial Influences on Weather and Climate,* B. M. McCormac, Ed., Colorado Associated University Press, 507–515.

Vautard, R., P. Yiou, and M. Ghil, 1992: Singular spectrum analysis: A toolkit for short noisy chaotic time series. *Physica D,* **58,** 95–126.

Wigley, T. M. L., and S. C. B. Raper, 1990: Climatic changes due to solar irradiance changes. *Geophys. Res. Lett.,* **17,** 2169–2172.